ASTRONOMY & ASTROPHYSICS
SUPPLEMENT SERIES

FEBRUARY I **1998**, PAGE 545

Astron. Astrophys. Suppl. Ser. **127,** 545-553 (1998)

Atomic data from the IRON Project

XXV. Electron impact excitation of fine-structure transitions in the ground configuration of Fe XII

A.M. Binello[1], **H.E. Mason**[1], **and P.J. Storey**[2]

[1] Department of Applied Mathematics and Theoretical Physics, University of Cambridge, Silver Street, Cambridge CB3 9EW, UK
[2] Department of Physics and Astronomy, University College London, Gower Street, London WC1 E6BT, UK

Received February 21; accepted February 21, 1997

Abstract. In the framework of the *IRON Project* we have performed new, fully quantum mechanical atomic calculations for the Fe XII (Fe^{11+}) coronal ion. Energy levels, oscillator strengths and spontaneous decay transition probabilities have been computed by including extensive configuration interaction (CI) and relativistic effects in the solution of the atomic structure problem. The R-matrix approach has been employed to solve the electron scattering problem and generate a new set of collisional atomic data. Results are discussed for the ten fine-structure forbidden transitions in the $3s^2\,3p^3$ ground configuration of Fe XII, and compared with previous calculations.

Key words: atomic data — atomic processes — Sun: corona — Sun: UV radiation

1. Introduction

The Solar Heliospheric Observatory (SOHO), an ESA/NASA space mission for the study of the solar upper chromosphere, transition region, inner and extended corona, was successfully launched in December, 1995. The analysis of SOHO spectra has generated a great deal of interest in the atomic physics related to coronal ions. In particular the *IRON Project*, an international collaboration aimed at providing the most accurate set of atomic data to date for all the iron ions (Hummer et al. 1993), is an ideal framework for the calculation of new atomic data for astrophysical applications. A complete list of IRON Project publications and papers in press can be found at http://www.am.qub.ac.uk. The Fe XII ion gives rise to spectral lines observed by several different spectrometers on board SOHO: at 195 Å (EIT – *Extreme ultraviolet Imaging Telescope*), at 1242 Å and 1349 Å (UVCS – *Ultraviolet Coronagraph and Spectrometer* and SUMER – *Solar Ultraviolet Measurement of Emitted Radiation*) and various lines in the CDS (*Coronal Diagnostic Spectrometer*) wavelength range 151 – 785 Å.

The first calculations for Fe XII were carried out by Flower (1977), who computed radiative and collisional data for transitions between the ground $3s^2\,3p^3$ and the first two excited $3s\,3p^4$ and $3s^2\,3p^2\,3d$ configurations. The *distorted wave* technique was employed in that work for the calculation of the scattering data. Bromage et al. (1978) and Fawcett (1986) provided improved excitation energies and oscillator strengths by incorporating strong CI (configuration interaction) and relativistic effects in the structure problem. Subsequently new and more extensive calculations were performed of energy levels and oscillator strengths for the same three lowest configurations (Tayal & Henry 1986) and of collision strengths, effective collision strengths and electron impact excitation rates for fine-structure transitions either within the ground $3s^2\,3p^3$ configuration (Tayal et al. 1987) or between this and the first excited $3s\,3p^4$ configuration (Tayal & Henry 1988). The use of these atomic data together with Fe XII lines identifications (Svensson 1971; Jordan 1971) has made possible a considerable amount of diagnostic work on physical parameters of the solar plasma. Electron temperature, density and iron abundance have been derived by analysing various spectra from early solar eclipse observations (Gabriel & Jordan 1975) to recent *Solar EUV Rocket Telescope and Spectrograph* SERTS (Thomas & Neupert 1994). The atomic data from Tayal & Henry (1986, 1988) and Tayal et al. (1987) are the most widely used in these astrophysical applications. However Mason (1994), in her assessment of theoretical electron excitation data for various iron ions, pointed out some unusual features in their Fe XII collisional data, which have not yet been explained. This has prompted the new set of atomic calculations which are described in this paper.

Send offprint requests to: A. Binello

Table 1. Configuration sets employed in the expansion of the Fe XII total wavefunction

set	configurations
1	$3s^2\,3p^3$, $3s\,3p^4$, $3s^2\,3p^2\,3d$, $3p^5$
2	set 1 + $3s\,3p^3\,3d$, $3p^4\,3d$, $3s\,3p^2\,3d^2$, $3p^3\,3d^2$, $3s^2\,3p\,3d^2$, $3s^2\,3d^3$, $3s\,3p\,3d^3$, $3p^2\,3d^3$
3	set 2 + $(3s^2\,3p^2)\,4s$, 4p, 4d, 4f; $(3s\,3p^3)\,4s$, 4p, 4d, 4f; $(3p^4)\,4s$, 4p, 4d, 4f
3A	same as set 3 but with 4s, 4p, 4d, 4f *correlation orbitals (hydrogenic)*

Table 2. Weighted oscillator strengths for the strongest Fe XII optically allowed transitions in LS coupling

Transition	set 1		set 2		set 3		set 3A	
	gf(L)	gf(V)	gf(L)	gf(V)	gf(L)	gf(V)	gf(L)	gf(V)
$3s^2\,3p^3\,{}^4S^o - 3s^2\,3p^2\,({}^3P)\,3d\,{}^4P$	8.048	4.459	6.203	5.723	6.076	5.794	6.116	5.702
$3s^2\,3p^3\,{}^2D^o - 3s\,3p^4\,{}^2P$	0.707	0.353	0.679	0.459	0.669	0.536	0.670	0.696
$3s^2\,3p^3\,{}^2D^o - 3s^2\,3p^2\,({}^3P)\,3d\,{}^2P$	3.225	1.563	2.414	2.210	2.396	2.193	2.373	2.238
$3s^2\,3p^3\,{}^2D^o - 3s^2\,3p^2\,({}^1D)\,3d\,{}^2D$	5.184	2.665	3.298	3.264	3.176	3.089	3.086	2.851
$3s^2\,3p^3\,{}^2D^o - 3s^2\,3p^2\,({}^3P)\,3d\,{}^2F$	10.431	6.108	7.978	7.637	7.805	7.769	7.870	7.291
$3s^2\,3p^3\,{}^2P^o - 3s\,3p^4\,{}^2S$	0.336	0.086	0.264	0.213	0.266	0.230	0.255	0.280
$3s^2\,3p^3\,{}^2P^o - 3s^2\,3p^2\,({}^1D)\,3d\,{}^2P$	3.200	2.107	2.532	2.084	2.498	2.229	2.465	2.119
$3s^2\,3p^3\,{}^2P^o - 3s^2\,3p^2\,({}^3P)\,3d\,{}^2D$	6.633	3.848	5.032	4.721	4.949	4.817	4.948	4.455

In Sect. 2 we discuss the atomic structure problem and the code used for the computation of the radiative data there presented. Section 3 will be devoted to the analysis of the $Fe^{11+} - e^-$ scattering problem and to the resulting collisional data relating to the fine-structure forbidden transitions within the ground $3s^2\,3p^3$ configuration. Corresponding results for allowed and intercombination transitions from the ground to the excited $3s\,3p^4$ and $3s^2\,3p^2\,3d$ configurations will be presented in a subsequent paper. Discussion and conclusions will be given in Sect. 4.

2. Atomic structure and radiative data

The atomic structure problem has been solved by employing the program *SUPERSTRUCTURE* (Eissner et al. 1974; Nussbaumer & Storey 1978), which has been developed over the years at University College London. This program uses multi-configuration expansions for the atomic eigenfunctions (CI). The structure and radiative calculations can be carried out in both LS coupling and intermediate coupling schemes. In the intermediate coupling case we diagonalise the Breit Pauli Hamiltonian, which includes the one-body and two-body relativistic operators, as specified in Eissner et al. (1974). The radial parts of the one electron wave-functions are calculated in scaled Thomas-Fermi-Dirac potentials. The scaling parameters, λ_{nl}, are chosen to minimise selected sets of LS coupled term energies.

The Fe^{11+} ion has a core $1s^2\,2s^2\,2p^6$ and five spectroscopically active electrons which occupy orbitals nl with $n \geq 3$ and $l = 0, \ldots, n-1$. We will be mostly interested in radiative data between the ground $3s^2\,3p^3$ odd-parity configuration and the first two excited $3s\,3p^4$, $3s^2\,3p^2\,3d$ even-parity configurations. However, it is necessary to include a greater number of more highly excited configurations, of both parities, in the wavefunctions basis set, in order to get accurate results. In Table 1 we list the configuration sets employed in different calculations to explore the accuracy of the wavefunction. For sets 1 to 3 we optimised the potential by minimising the energies of all the terms included in the expansion, therefore obtaining orbitals all of spectroscopic type. For set 3A the minimisation was done on 20 LS coupling terms only, those belonging to the $3s^2\,3p^3$, $3s\,3p^4$ and $3s^2\,3p^2\,3d$ configurations. In such a way we could study the effects of using 4s, 4p, 4d and 4f correlation orbitals, all taken of hydrogenic nature (a similar calculation carried out with a 4f Thomas-Fermi correlation orbital led to identical conclusions). These correlation orbitals are approximations to the real orbitals, introduced in order to allow for correlation with the missing configurations in the basis set, and can be highly contracted compared to the spectroscopic ones. The scaling parameters for the potential employed in the set 3A calculation are $\lambda_{1s} = 1.41049$, $\lambda_{2s} = 1.12071$, $\lambda_{2p} = 1.06116$, $\lambda_{3s} = 1.14871$, $\lambda_{3p} = 1.13081$, $\lambda_{3d} = 1.16752$, $\lambda_{4s} = 1.35037$, $\lambda_{4p} = 1.30434$, $\lambda_{4d} = 1.16657$, $\lambda_{4f} = 0.84416$. The wavefunctions obtained in the different computations have been used to calculate the length f(L) and velocity f(V) forms of the oscillator strength for transitions between LS coupling terms or intermediate

coupling fine-structure levels. The agreement between the two forms and their stability as more configurations are added to the basis set are used as an indicator of the quality of the computation. In Table 2 we present results for the two forms of the oscillator strength, weighted with the statistical weight of the initial level, for selected optically allowed transitions in LS coupling between the ground and the first two excited configurations in Fe XII, for the basis sets illustrated above.

The first point of interest is the clear improvement in going from the coarse 4 configuration model (set 1) to the much more comprehensive set including $n = 4$ electrons (set 3), as testified by the closer agreement of the gf(L) and gf(V) values. Correlation effects introduced by the $n = 4$ correlation orbitals (set 3A) do not consistently improve the results and any improvement is often only marginal.

There is however considerably better agreement between theoretical and observed energy levels when correlation orbitals are used, as can be seen in Table 3. We therefore regard the set 3A as our best approximation, as far as the provision of structure and radiative data is concerned. Another important point is apparent in the magnitude of several values of gf(L) for transitions from terms of the $3s^2\,3p^2\,3d$ excited configuration down to the $3s^2\,3p^3$ configuration. Clearly radiative cascades from those levels are extremely important in populating the levels of the ground configuration. The availability of accurate collisional data for the population mechanisms of $3s^2\,3p^2\,3d$ levels is therefore a key issue, which will be stressed in the next section. In Table 3 we present the list of fine-structure levels for the three energetically lowest configurations of Fe XII, along with calculated and observed energy values. Theoretical energies are those obtained with our set 3 and set 3A models. Experimental values have been taken from the compilation by Corliss & Sugar (1982) and, where available, from the updated list by Jupen et al. (1993). The average difference between theoretical (set 3A) and observed values was found to be 2.7% for the ground $3s^2\,3p^3$ configuration, 0.6% for the $3s\,3p^4$ configuration and 2.2% for the $3s^2\,3p^2\,3d$ configuration. The improvement of our computation over previous works is shown by the comparison with corresponding results by Flower (1977) (5.5%, 1.7% and 3.3% respectively) and by Tayal & Henry (1986) (3.7%, 1.4% and 4.2%). For the lowest twelve levels of the $3s^2\,3p^2\,3d$ configuration experimental energies are not yet available. In order to fill this gap we used theoretical energies that were empirically corrected by adding the weighted average of the difference $E_{\rm obs} - E_{\rm th}$ for other levels in the same configuration having the same parent term, whose energies are experimentally known. These estimates are distinguished by italic type in the column listing the experimental values. Finally in Table 4 we show weighted oscillator strengths, calculated with our set 3A model, for selected electric dipole transitions between fine-structure levels in intermediate coupling. There is generally a good agreement between these data, the corresponding values from Tayal & Henry (1986) and, in particular, those from Bromage et al. (1978). As in the latter work the authors performed empirical adjustments on the Slater parameters in order to minimise discrepancies between computed and measured energy levels, we regard the particularly good agreement with their oscillator strengths as highly satisfactory.

Table 3. Energy levels (cm^{-1}) for the lowest three configurations in Fe XII. For values in *italic* see text

Configuration	Level	$E_{\rm th}$ (set 3)	$E_{\rm th}$ (set 3A)	$E_{\rm obs}$
$3s^2\,3p^3$	$^4S^o_{3/2}$	0	0	0
	$^2D^o_{3/2}$	44477	42789	41555
	$^2D^o_{5/2}$	49049	46907	46088
	$^2P^o_{1/2}$	77755	76895	74108
	$^2P^o_{3/2}$	84059	82587	80515
$3s\,3p^4$	$^4P_{5/2}$	274093	274389	274373
	$^4P_{3/2}$	283799	283883	284005
	$^4P_{1/2}$	288194	288235	288307
	$^2D_{3/2}$	343277	341900	339761
	$^2D_{5/2}$	345171	343595	341703
	$^2P_{3/2}$	396678	394281	389668
	$^2P_{1/2}$	401278	399595	394352
	$^2S_{1/2}$	417216	415694	410401
$3s^2\,3p^2\,3d$	$(^3P)\,^4F_{3/2}$	435809	431849	*420258*
	$(^3P)\,^4F_{5/2}$	439573	435616	*424022*
	$(^3P)\,^4F_{7/2}$	445081	441131	*429530*
	$(^3P)\,^4F_{9/2}$	451936	447979	*436385*
	$(^1D)\,^2F_{5/2}$	452611	449292	*437194*
	$(^3P)\,^4D_{1/2}$	455867	452638	*440316*
	$(^3P)\,^4D_{7/2}$	456492	453159	*440941*
	$(^3P)\,^4D_{3/2}$	456966	453713	*441414*
	$(^3P)\,^4D_{5/2}$	461606	458342	*446055*
	$(^1D)\,^2F_{7/2}$	471304	468104	*455887*
	$(^1D)\,^2G_{7/2}$	507320	503510	*491903*
	$(^1D)\,^2G_{9/2}$	510296	506378	*494879*
	$(^3P)\,^2P_{3/2}$	513685	511268	501800
	$(^3P)\,^4P_{5/2}$	524880	521908	512510
	$(^3P)\,^2P_{1/2}$	525739	523255	513850
	$(^3P)\,^4P_{3/2}$	528938	526123	516740
	$(^3P)\,^4P_{1/2}$	531540	528826	519770
	$(^1S)\,^2D_{3/2}$	539623	537312	526120
	$(^1S)\,^2D_{5/2}$	550427	547826	538040
	$(^1D)\,^2D_{3/2}$	567870	565364	554030
	$(^1D)\,^2D_{5/2}$	569025	566648	554610
	$(^1D)\,^2P_{1/2}$	587307	586413	568940
	$(^3P)\,^2F_{5/2}$	593418	590771	576740
	$(^1D)\,^2P_{3/2}$	595306	594486	577740
	$(^1D)\,^2S_{1/2}$	593956	592965	579630
	$(^3P)\,^2F_{7/2}$	597798	595133	581180
	$(^3P)\,^2D_{5/2}$	621026	618968	603930
	$(^3P)\,^2D_{3/2}$	622632	620649	605480

Table 4. Weighted oscillator strengths for Fe XII electric dipole transitions in intermediate coupling

Transition	gf(L)		
	present work (set 3A)	Bromage et al. (1978)	Tayal & Henry (1986)
$3s^2\,3p^3\ {}^4S^o_{3/2} - 3s\,3p^4\ {}^4P_{5/2}$	0.190	0.190	0.212
$3s^2\,3p^3\ {}^4S^o_{3/2} - 3s\,3p^4\ {}^4P_{3/2}$	0.128	0.130	0.144
$3s^2\,3p^3\ {}^4S^o_{3/2} - 3s\,3p^4\ {}^4P_{1/2}$	0.065	0.065	0.072
$3s^2\,3p^3\ {}^4S^o_{3/2} - 3s^2\,3p^2\,3d\ ({}^3P){}^4P_{5/2}$	3.012	3.190	
$3s^2\,3p^3\ {}^4S^o_{3/2} - 3s^2\,3p^2\,3d\ ({}^3P){}^4P_{3/2}$	2.035	2.13	
$3s^2\,3p^3\ {}^4S^o_{3/2} - 3s^2\,3p^2\,3d\ ({}^3P){}^4P_{1/2}$	0.995	1.01	
$3s^2\,3p^3\ {}^4S^o_{3/2} - 3s^2\,3p^2\,3d\ ({}^1S){}^2D_{5/2}$	0.081	0.082	0.142
$3s^2\,3p^3\ {}^2D^o_{3/2} - 3s\,3p^4\ {}^2D_{3/2}$	0.225	0.230	0.256
$3s^2\,3p^3\ {}^2D^o_{3/2} - 3s\,3p^4\ {}^2P_{1/2}$	0.177	0.170	0.188
$3s^2\,3p^3\ {}^2D^o_{3/2} - 3s^2\,3p^2\,3d\ ({}^3P){}^2P_{3/2}$	0.535	0.54	0.484
$3s^2\,3p^3\ {}^2D^o_{3/2} - 3s^2\,3p^2\,3d\ ({}^3P){}^2P_{1/2}$	0.591	0.61	0.628
$3s^2\,3p^3\ {}^2D^o_{3/2} - 3s^2\,3p^2\,3d\ ({}^1D){}^2D_{3/2}$	1.330	1.520	1.428
$3s^2\,3p^3\ {}^2D^o_{3/2} - 3s^2\,3p^2\,3d\ ({}^1D){}^2D_{5/2}$	0.079	0.080	0.040
$3s^2\,3p^3\ {}^2D^o_{3/2} - 3s^2\,3p^2\,3d\ ({}^3P){}^2F_{5/2}$	3.22	3.39	
$3s^2\,3p^3\ {}^2D^o_{5/2} - 3s\,3p^4\ {}^2D_{5/2}$	0.285	0.280	0.324
$3s^2\,3p^3\ {}^2D^o_{5/2} - 3s\,3p^4\ {}^2P_{3/2}$	0.388	0.420	0.438
$3s^2\,3p^3\ {}^2D^o_{5/2} - 3s^2\,3p^2\,3d\ ({}^3P){}^2P_{3/2}$	1.336	1.380	1.374
$3s^2\,3p^3\ {}^2D^o_{5/2} - 3s^2\,3p^2\,3d\ ({}^1S){}^2D_{3/2}$	0.162	0.160	0.078
$3s^2\,3p^3\ {}^2D^o_{5/2} - 3s^2\,3p^2\,3d\ ({}^1S){}^2D_{5/2}$	1.166	1.120	1.038
$3s^2\,3p^3\ {}^2D^o_{5/2} - 3s^2\,3p^2\,3d\ ({}^3P){}^2F_{7/2}$	4.581	4.820	
$3s^2\,3p^3\ {}^2D^o_{5/2} - 3s^2\,3p^2\,3d\ ({}^3P){}^2D_{5/2}$	0.135	0.130	
$3s^2\,3p^3\ {}^2P^o_{1/2} - 3s\,3p^4\ {}^2P_{1/2}$	0.095	0.098	0.116
$3s^2\,3p^3\ {}^2P^o_{1/2} - 3s^2\,3p^2\,3d\ ({}^3P){}^2P_{1/2}$	0.131	0.100	0.150
$3s^2\,3p^3\ {}^2P^o_{1/2} - 3s^2\,3p^2\,3d\ ({}^1D){}^2D_{3/2}$	0.176	0.150	0.198
$3s^2\,3p^3\ {}^2P^o_{1/2} - 3s^2\,3p^2\,3d\ ({}^1D){}^2P_{1/2}$	0.810	0.890	
$3s^2\,3p^3\ {}^2P^o_{1/2} - 3s^2\,3p^2\,3d\ ({}^1D){}^2P_{3/2}$	0.450	0.500	
$3s^2\,3p^3\ {}^2P^o_{3/2} - 3s\,3p^4\ {}^2D_{5/2}$	0.073	0.072	0.088
$3s^2\,3p^3\ {}^2P^o_{3/2} - 3s\,3p^4\ {}^2S_{1/2}$	0.202	0.180	0.224
$3s^2\,3p^3\ {}^2P^o_{3/2} - 3s^2\,3p^2\,3d\ ({}^3P){}^2P_{3/2}$	0.158	0.130	0.176
$3s^2\,3p^3\ {}^2P^o_{3/2} - 3s^2\,3p^2\,3d\ ({}^3P){}^2P_{1/2}$	0.231	0.200	0.248
$3s^2\,3p^3\ {}^2P^o_{3/2} - 3s^2\,3p^2\,3d\ ({}^1D){}^2S_{1/2}$	0.764	0.780	
$3s^2\,3p^3\ {}^2P^o_{3/2} - 3s^2\,3p^2\,3d\ ({}^3P){}^2D_{5/2}$	3.036	3.310	
$3s^2\,3p^3\ {}^2P^o_{3/2} - 3s^2\,3p^2\,3d\ ({}^3P){}^2D_{3/2}$	0.495	0.500	

3. The $Fe^{11+} - e^-$ scattering problem

For the solution of the $Fe^{11+} - e^-$ inelastic scattering problem we employed the *R-matrix* technique (Burke et al. 1971; Berrington et al. 1987; Burke & Berrington 1993; Hummer et al. 1993). This method has been implemented in the Queen's University Belfast R-matrix suite of programs, the latest and most updated version of which is thoroughly described in Berrington et al. (1995).

The scattering calculation is carried out in LS coupling, but the mass and Darwin relativistic energy corrections are included (Saraph & Storey 1996). The transformation to pair coupling including the effects of intermediate coupling in the target are included as discussed in the first IRON Project paper (Hummer et al. 1993).

Two sets of R-matrix calculations have been performed in order to analyse critically previous computations and to provide new electron scattering data for Fe XII. These will be described in the two following subsections.

3.1. 7 term R-matrix computation

Our initial set of R-matrix calculations was aimed at studying the effect of varying target representations on collisional data and, in particular, on the resonance structure of the collision strengths below the highest excitation threshold in the target. As in Tayal et al. (1987) the lowest seven LS coupling terms, $3s^2\,3p^3\ {}^4S^o$, ${}^2D^o$, ${}^2P^o$, $3s\,3p^4$ ${}^4P$, ${}^2D$, ${}^2P$, ${}^2S$, were included in the expansion of the total wavefunction for the target. The energies for these excitation thresholds were calculated as averages of observed

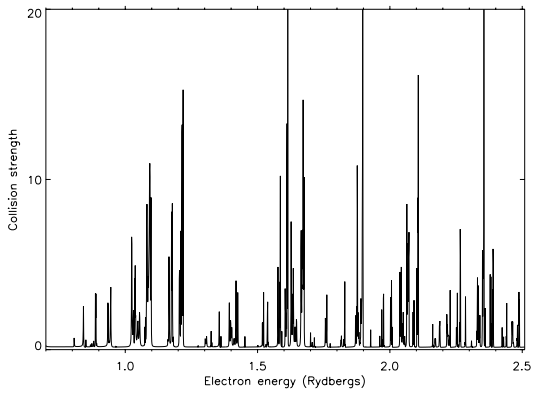

Fig. 1. Collision strength for Fe XII forbidden transition $3s^2\,3p^3\ {}^2D^o_{3/2} - {}^2\,D^o_{5/2}$. R-matrix calculation including 7 LS coupling target terms with $\overline{3}d_{TF}$ correlation orbital

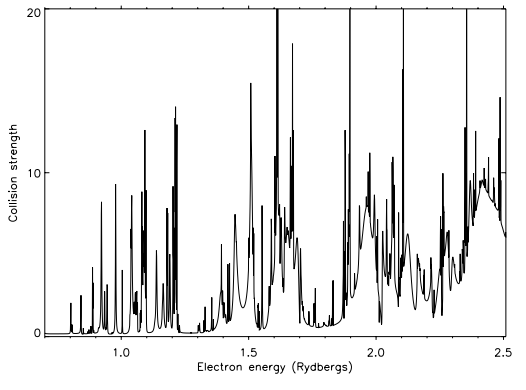

Fig. 2. Collision strength for Fe XII forbidden transition $3s^2\,3p^3\ {}^2D^o_{3/2} - {}^2\,D^o_{5/2}$. R-matrix calculation including 7 LS coupling target terms with $\overline{3}d_{TF}$, $\overline{4}f_{Hy}$ correlation orbitals

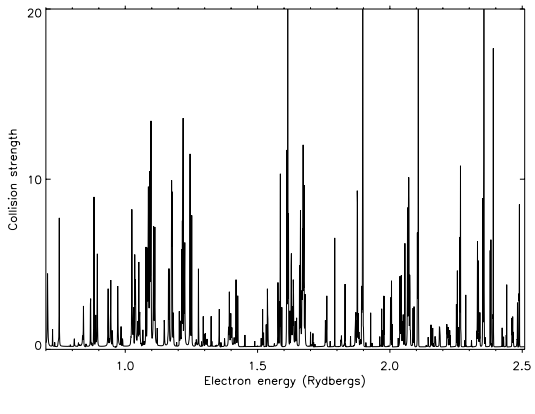

Fig. 3. Collision strength for Fe XII forbidden transition $3s^2\,3p^3\ {}^2D^o_{3/2} - {}^2\,D^o_{5/2}$. R-matrix calculation including 7 LS coupling target terms with 3d, 4f spectroscopic orbitals

Table 5. LS coupling target terms included in our R-matrix calculations

Configuration	Term	E(Ry)
$3s^2\,3p^3$	$^4S^o$	0.0
	$^2D^o$	0.40346
	$^2P^o$	0.71424
$3s\,3p^4$	^4P	2.55069
	^2D	3.10674
	^2P	3.56514
	^2S	3.73984
$3s^2\,3p^2\,3d$	$(^3P)\,^4F$	*3.91364*
	$(^3P)\,^4D$	*4.03242*
	$(^1D)\,^2F$	*4.08134*
	$(^1D)\,^2G$	*4.49761*
	$(^3P)\,^2P$	4.60933
	$(^3P)\,^4P$	4.69420
	$(^1S)\,^2D$	4.85952
	$(^1D)\,^2D$	5.05186
	$(^1D)\,^2S$	5.22953
	$(^1D)\,^2P$	5.23802
	$(^3P)\,^2F$	5.27875
	$(^3P)\,^2D$	5.50906

values, weighted over the fine-structure levels, and are tabulated as the first seven entries in Table 5. Experimental energies were preferred to theoretical values in order to determine as accurately as possible the positions of the convergence limits for Rydberg series of resonances. The seven target terms were represented by CI expansions constructed with a common set of radial functions, describing the radial charge distribution of the target. Three different combinations of seven orthogonal one-electron orbitals 1s, 2s, 2p, 3s, 3p, 3d and 4f were selected, in order to match as closely as possible the details of Tayal et al. (1987) calculation. In the first computation radial waves were obtained in the way described in Sect. 2 by including nine configurations in the basis set, $3s^2\,3p^3$, $3s\,3p^4$, $3s^2\,3p^2\,\overline{3}d$, $3p^5$, $3s\,3p^2\,\overline{3}d^2$, $3p^3\,\overline{3}d^2$, $3s\,3p^3\,\overline{3}d$, $3p^4\,\overline{3}d$, $3s^2\,3p\,\overline{3}d^2$, where the $\overline{3}d$ correlation orbital was chosen of Thomas-Fermi type ($\overline{3}d_{TF}$). The bar over the principal quantum number n indicates the correlation nature of the orbital. In the second calculation we added the two extra configurations $3s^2\,3p^2\,\overline{4}f$ and $3s\,3p^3\,\overline{4}f$ to the basis set, hence investigating the effect of a $\overline{4}f$ correlation orbital of hydrogenic type ($\overline{4}f_{Hy}$). In these two calculations the size of the R-matrix "box", within which exchange and e−e correlation interactions are treated explicitly by performing a CI expansion of the $(N+1)-$e collision complex wavefunction, was set at $a = 3.22$ a.u. and 16 continuum orbitals were included to ensure convergence for electron energies spanning the range 0.4 to 100 Ry. In our third calculation the same set of eleven configurations was kept in the basis expansion, but this time with 3d and 4f orbitals of spectroscopic type.

Due to the presence of a diffuse 4f spectroscopic orbital, compared to the more contracted correlation type equivalent (see Table 6), it was necessary to increase a to 5.34 a.u. and to include a total of 24 continuum orbitals in the problem. The wavefunction for the $(N+1)-$e collision complex was, in all three cases, expanded on a basis set of 72 intermediate states, including partial waves of singlet, triplet and quintet spin multiplicities, both odd and even parities and with total orbital angular momenta L from 0 to 12, which corresponds to an expansion in intermediate coupling with values of $J = L + S$ from 0 to 10. The variation of the collision strength, as a function of electron energy, with target structure is presented in the three plots of Fig. 1, Fig. 2 and Fig. 3, corresponding to the three calculations described above. Here collision strengths for the fine-structure forbidden transition $3s^2\,3p^3\ {}^2D^o_{3/2} - {}^2D^o_{5/2}$ are plotted in the energy region between the $3s^2 3p^3\ {}^2P^o_{3/2}$ and $3s\,3p^4\ {}^4P_{5/2}$ target thresholds, revealing the complicated pattern of different series of resonances. A very fine energy mesh of $9.0508\,10^{-4}$ Ry was chosen to delineate this complex resonance structure. Clearly it is the correlation nature of the $\overline{4}$f orbital which introduces the broad resonant features visible in Fig. 2. This important point will be further discussed in Sect. 4.

3.2. 19 term R-matrix computation

A higher quality set of collisional data for Fe XII was obtained by increasing the size of the expansion for both the target and the $(N+1)-$e system total wavefunctions. In a new, ab initio R-matrix calculation we extended the target representation by including in the target the 12 LS coupling terms of the $3s^2\,3p^2\,3d$ configuration, $(^3P)\,{}^4F$, $(^3P)\,{}^4D$, $(^1D)\,{}^2F$, $(^1D)\,{}^2G$, $(^3P)\,{}^2P$, $(^3P)\,{}^4P$, $(^1S)\,{}^2D$ $(^1D)\,{}^2D$, $(^1D)\,{}^2S$, $(^1D)\,{}^2P$, $(^3P)\,{}^2F$, $(^3P)\,{}^2D$. The list of energies for the total set of 19 LS coupling target terms employed in this calculation is given in Table 5. The lowest four energy values for the $3s^2\,3p^2\,3d$ configuration (italic type) have been calculated from the corrected level energies presented in Table 3, due to lack of observed energies for the corresponding fine-structure levels, as discussed in Sect. 2. It should be noted that the energy value for the $3s^2\,3p^2\,3d\ (^1D)\,{}^2S$ term in Table 5 does not correspond to the experimental energy given in Table 3. This observed value was modified in order to preserve the theoretical ordering of the term energies, as determined by the R-matrix computer code, where the $(^1D)\,{}^2S$ term falls in between the $(^1D)\,{}^2D$ and $(^1D)\,{}^2P$ terms. Failing to preserve the theoretical ordering can lead to indexing problems in the R-matrix program. The correction was taken as the difference between the calculated and experimental energy values for the $(^1D)\,{}^2P$ term. The radial waves describing the distribution of the bound electrons in the target were obtained with the twelve configuration basis of set 2 in Table 1. This represented a good compromise between target quality and computational speed. The scaling parameters for the potential employed in the set 2 structure calculation are $\lambda_{1s} = 1.41337$, $\lambda_{2s} = 1.11538$, $\lambda_{2p} = 1.06220$, $\lambda_{3s} = 1.13461$, $\lambda_{3p} = 1.10992$, $\lambda_{3d} = 1.13567$. A total of 16 continuum orbitals was included and the inner region boundary was set at 3.09 a.u. An initial expansion of the $(N+1)-$e system total wavefunction on a basis set including partial waves with total angular momenta $J \leq 10$ turned out to be insufficient to ensure convergence of the collision strengths for some of the forbidden transitions at high electron energies. The final 19 state calculation was therefore carried out for all partial waves with $J \leq 15$, again for both odd and even parities and singlet, triplet and quintet spin states, including a total of 102 intermediate states. In Fig. 4 we present results for the same transition illustrated in Fig. 1, this time spanning the whole closed channel energy range, going from the lowest $(3s^2\,3p^3\ {}^2D^o_{3/2})$ to the highest $(3s^2\,3p^2\,3d\ {}^2D_{3/2})$ excitation threshold.

The rapidly varying behaviour of the collision strength as a function of electron energy is again noticeable, this time enriched by the additional series of resonances converging to the extra thresholds belonging to the $3s^2\,3p^2\,3d$ configuration. A top-up procedure to estimate the contributions to the collision strengths from partial waves with $J > 15$ was adopted in the open channel energy region, above the highest excitation threshold. By assuming that the partial collision strengths form a geometric series with a geometric scaling factor equal to the ratio of the last two adjacent terms explicitly included, we obtain for the contribution, S, from $J > 15$

$$S = \frac{x\,\Omega_{J=15}}{1-x} \qquad \text{where} \qquad x = \frac{\Omega_{J=15}}{\Omega_{J=14}}\,. \tag{1}$$

This top-up procedure was found to be appropriate for the ten optically forbidden transitions within the ground $3s^2\,3p^3$ configuration, with a maximum correction for $J = 16 \rightarrow \infty$ of 15% at the highest electron energy considered (100 Ry). At the lowest energy in the open channel region (6 Ry) the maximum correction due to $J > 15$ is found to be 1.4%. Below 6 Ry, no top-up is considered necessary.

However for the optically allowed transitions the contribution from $J > 15$ predicted by Eq. (1) is much larger ($\simeq 100\%$). Alternative top-up techniques are needed and results for these transitions will be presented elsewhere. Final collision strength values $\Omega\,(i \rightarrow j)$ for the forbidden transitions between the five levels of the $3s^2\,3p^3$ ground configuration are presented in Table 7, on a grid of energy points above the highest excitation threshold.

Electron excitation rates, obtained by averaging collision cross sections over a Maxwellian distribution of electron energies, are better represented in terms of *effective* (or *thermally averaged*) collision strengths, given by

$$\Upsilon\,(i \rightarrow j) = \int_0^\infty \Omega\,(i \rightarrow j) \exp\left(-\frac{E_j}{kT_e}\right) \mathrm{d}\left(\frac{E_j}{kT_e}\right) \tag{2}$$

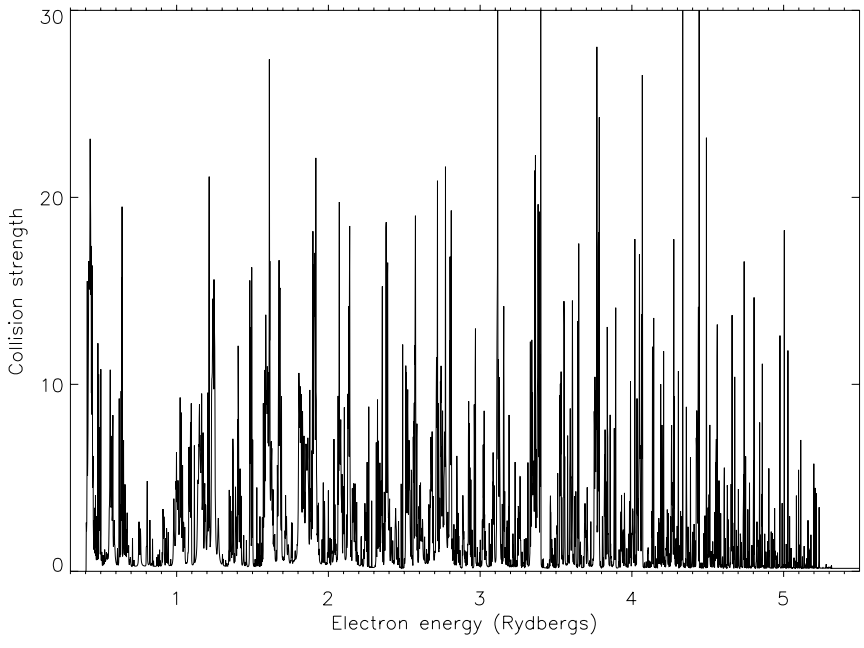

Fig. 4. Collision strength for Fe XII forbidden transition $3s^2\,3p^3\ {}^2D^o_{3/2} - {}^2D^o_{5/2}$. *R*-matrix calculation including 19 *LS* coupling target terms

Table 6. Mean radii $< r >$ of 3d and 4f orbitals for different combinations of 3d, 4f orbitals

Orbital	3d, 4f spectroscopic	$\overline{3}d_{TF}$, $\overline{4}f_{Hy}$	$\overline{3}d_{TF}$, $\overline{4}f_{TF}$	$\overline{3}d_{Hy}$, $\overline{4}f_{Hy}$	$\overline{3}d_{Hy}$, $\overline{4}f_{TF}$
3d	0.68862	0.69790	0.69789	0.67926	0.67929
4f	1.42519	0.83966	0.84152	0.83838	0.83985

Table 7. Collision strengths for fine-structure forbidden transitions within the $3s^2\,3p^3$ ground configuration of Fe XII

Transition	E (Ry)						
	6.5	10	15	20	30	50	100
$^4S^o_{3/2} - {}^2D^o_{3/2}$	0.055	0.047	0.038	0.032	0.024	0.016	0.011
$^4S^o_{3/2} - {}^2D^o_{5/2}$	0.086	0.073	0.061	0.052	0.041	0.030	0.021
$^4S^o_{3/2} - {}^2P^o_{1/2}$	0.009	0.007	0.005	0.004	0.003	0.001	0.001
$^4S^o_{3/2} - {}^2P^o_{3/2}$	0.017	0.013	0.009	0.007	0.004	0.002	0.001
$^2D^o_{3/2} - {}^2D^o_{5/2}$	0.170	0.153	0.136	0.125	0.111	0.098	0.088
$^2D^o_{3/2} - {}^2P^o_{1/2}$	0.295	0.291	0.286	0.288	0.286	0.290	0.290
$^2D^o_{3/2} - {}^2P^o_{3/2}$	0.203	0.197	0.191	0.190	0.187	0.186	0.186
$^2D^o_{5/2} - {}^2P^o_{1/2}$	0.223	0.219	0.214	0.215	0.213	0.215	0.216
$^2D^o_{5/2} - {}^2P^o_{3/2}$	0.675	0.665	0.652	0.655	0.650	0.656	0.658
$^2P^o_{1/2} - {}^2P^o_{3/2}$	0.068	0.062	0.055	0.050	0.045	0.040	0.036

Table 8. Effective collision strengths for fine-structure forbidden transitions within the $3s^2\,3p^3$ ground configuration of Fe XII. Temperatures in the range $4\,10^5\,\mathrm{K} - 3\,10^6\,\mathrm{K}$

Transition	T_e (10^5 K)										
	4	6	8	10	12	14	16	18	20	25	30
$^4S^o_{3/2} - {}^2D^o_{3/2}$	0.268	0.227	0.196	0.174	0.157	0.143	0.132	0.123	0.115	0.100	0.088
$^4S^o_{3/2} - {}^2D^o_{5/2}$	0.268	0.233	0.207	0.187	0.171	0.158	0.148	0.139	0.131	0.117	0.106
$^4S^o_{3/2} - {}^2P^o_{1/2}$	0.074	0.063	0.055	0.048	0.043	0.039	0.035	0.032	0.030	0.025	0.022
$^4S^o_{3/2} - {}^2P^o_{3/2}$	0.304	0.257	0.219	0.190	0.168	0.150	0.136	0.124	0.114	0.096	0.082
$^2D^o_{3/2} - {}^2D^o_{5/2}$	2.375	1.989	1.699	1.482	1.315	1.184	1.078	0.991	0.918	0.778	0.680
$^2D^o_{3/2} - {}^2P^o_{1/2}$	0.763	0.679	0.617	0.570	0.535	0.507	0.485	0.466	0.451	0.423	0.403
$^2D^o_{3/2} - {}^2P^o_{3/2}$	1.418	1.236	1.084	0.966	0.874	0.800	0.740	0.691	0.650	0.570	0.514
$^2D^o_{5/2} - {}^2P^o_{1/2}$	0.556	0.490	0.444	0.411	0.385	0.366	0.350	0.337	0.327	0.307	0.293
$^2D^o_{5/2} - {}^2P^o_{3/2}$	1.779	1.572	1.421	1.311	1.227	1.162	1.110	1.068	1.032	0.966	0.919
$^2P^o_{1/2} - {}^2P^o_{3/2}$	1.241	1.082	0.940	0.826	0.736	0.663	0.604	0.555	0.514	0.434	0.378

Table 9. Effective collision strengths for fine-structure forbidden transitions within the $3s^2\,3p^3$ ground configuration of Fe XII. Temperatures in the range $4\,10^6\,\mathrm{K} - 10^7\,\mathrm{K}$. For values in *italic* see text

Transition	T_e (10^6 K)						
	4	5	6	7	8	9	10
$^4S^o_{3/2} - {}^2D^o_{3/2}$	0.0732	0.0631	0.0559	0.0505	0.0463	0.0429	*0.0401*
$^4S^o_{3/2} - {}^2D^o_{5/2}$	0.0901	0.0796	0.0720	0.0663	0.0617	*0.0580*	*0.0549*
$^4S^o_{3/2} - {}^2P^o_{1/2}$	0.0175	0.0147	0.0126	0.0111	0.0100	0.0090	0.0083
$^4S^o_{3/2} - {}^2P^o_{3/2}$	0.0642	0.0529	0.0450	0.0392	0.0347	0.0312	0.0283
$^2D^o_{3/2} - {}^2D^o_{5/2}$	0.5487	0.4655	0.4080	0.3658	0.3335	0.3079	*0.2872*
$^2D^o_{3/2} - {}^2P^o_{1/2}$	0.3764	0.3600	*0.3488*	*0.3407*	*0.3345*	*0.3297*	*0.3258*
$^2D^o_{3/2} - {}^2P^o_{3/2}$	0.4399	0.3929	0.3606	*0.3370*	*0.3190*	*0.3048*	*0.2934*
$^2D^o_{5/2} - {}^2P^o_{1/2}$	0.2751	0.2638	*0.2561*	*0.2505*	*0.2463*	*0.2430*	*0.2403*
$^2D^o_{5/2} - {}^2P^o_{3/2}$	0.8580	0.8199	*0.7940*	*0.7752*	*0.7609*	*0.7497*	*0.7407*
$^2P^o_{1/2} - {}^2P^o_{3/2}$	0.3020	0.2538	0.2205	0.1960	0.1773	0.1625	0.1505

where E_j is the colliding electron kinetic energy relative to the upper level j of the transition. We have integrated our collision strengths using the linear interpolation technique described in Burgess & Tully (1992) and results are tabulated in Table 8 and Table 9 for two different temperature ranges. In integrating the collision strengths we made the assumption $\Omega\,(100\,\mathrm{Ry} < E < \infty) = \Omega\,(100\,\mathrm{Ry})$, i.e. constant Ω at energies above the last calculated point. The contribution coming from this energy region to the total $\Upsilon\,(T_e)$ increases with T_e and is generally $< 5\%$. When it is $> 5\%$ we used italic type in Table 9. For the transitions $^2D^o - {}^2P^o$, in particular, this contribution can be as high as 18% at the highest temperatures. However, from Table 7 we see that the assumption of constant $\Omega\,(E)$ at high energies, particularly for the transitions $^2D^o - {}^2P^o$, is excellent.

4. Discussion and conclusions

Two major anomalies affect the collisional data computed by Tayal et al. (1987) for the forbidden transitions within the $3s^2\,3p^3$ ground configuration of Fe XII

1. a large discontinuity, up to an order of magnitude for some transitions, between the Ω values at 4 Ry and at 6.6 Ry, as clear from their Table 2. This feature was pointed out by Mason (1994).
2. a monotonic increase of Ω as a function of E above 6.6 Ry for the transitions from the $^2D^o_J$ up to the $^2P^o_J$ levels.

Comparison of our Figs. 1, 2 and 3 with their Fig. 3 shows that our 7 term target expansion including $\overline{3}$d and $\overline{4}$f correlation orbitals in the radial waves (Fig. 2) is the closest to their model.

Regarding the first point, we note that 4 Ry is above the highest excitation threshold in both calculations, so the eventuality of hitting a true resonance at that energy

must be ruled out. This raises the question whether their unusually high values at 4 Ry might be due to the effect of unphysical resonances in the open channel energy region, despite their use of a T-matrix smoothing procedure in that energy range. Our 7 term computation with correlation orbitals revealed a bunch of resonances, likely to be due to the $\overline{4}$f correlation orbital, between 4 Ry and 7 Ry, and between 15 Ry and 20 Ry. Our approach does not include T-smoothing but we still find the same steep drop in the Ω values between 4 Ry and 6.6 Ry. This fact seems to suggest that open channel resonance effects are still affecting their non-resonant background, causing this behaviour.

As far as the second point is concerned, they ascribe the increase in Ω to larger contributions from higher partial waves due to the presence of stronger long-range quadrupole interactions. However we performed a similar top-up procedure without obtaining such a pronounced effect in the higher partial waves contributions. Furthermore we point out that, according to the classification proposed by Burgess & Tully (1992), the high energy behaviour of $\Omega(E)$ for forbidden transitions should follow a constant or E^{-2} trend, depending on the role played by electron exchange. An increase in Ω with E is, on the contrary, typical of optically allowed transitions.

The use of correlation orbitals in the target description is problematic, as stated in Saraph & Storey (1996), because of the introduction of unwanted spurious resonances in the open channel region and because of the inaccurate position on the energy scale of the additional resonances brought in by these non-physical orbitals below the highest excitation threshold. It is for this reason that we used all spectroscopic orbitals in our best R-matrix calculation including 19 target terms. A comparison of our Table 7 with the Tayal et al. (1987) collision strengths reveals a situation where their values are, for most transitions, larger than ours. The use of a different scaling factor in the geometric series top-up procedure and possible residual open channel resonance effects in their data might account for this discrepancy. However, no clear pattern is observed in comparing the two sets of data for the effective collision strengths (our Table 8 and their Table 3). Their $\Upsilon(T_e)$ data for the $^2D^o_J - ^2P^o_J$ transitions show again the same anomalous behaviour as a function of T_e as we found in their $\Omega(E)$ values. Here, probably, in integrating the collision strengths over a Maxwellian distribution, the presence of their broad resonance features due to correlation orbitals is balanced by our inclusion of additional series of physical resonances converging to the twelve extra thresholds of the $3s^2\,3p^2\,3d$ configuration, which is lacking in their target representation. The inclusion of the second excited configuration in the target expansion is an important feature of our calculation because it enables us to provide collisional data for the important transitions up to the $3s^2\,3p^2\,3d$ levels. The only set of data previously available for these transitions was by Flower (1977), who used a very crude target model and included resonance effects by the approximate method of Petrini (1970). The radiative and collisional atomic parameters for Fe XII discussed in this paper should therefore prove a powerful diagnostic tool for future spectroscopic applications.

Acknowledgements. This research was supported by PPARC grants GR/H94979 and GR/K98506 for the IRON Project meetings and CRAY computing time.

References

Berrington K.A., Burke P.G., Butler K., Seaton M.J., Storey P.J., Taylor K.T., Yu Yan, 1987, J. Phys. B 20, 6379
Berrington K.A., Eissner W.B., Norrington P.H., 1995, Computer Phys. Commun. 92, 290
Bromage G.E., Cowan R.D., Fawcett B.C., 1978, MNRAS 183, 19
Burgess A., Tully J.A., 1992, A&A 254, 436
Burke P.G., Berrington K.A., 1993, Atomic and molecular processes: an R-matrix approach. Institute of Physics Publishing, Bristol and Philadelphia, p. 1
Burke P.G., Hibbert A., Robb W.D., 1971, J. Phys. B 4, 153
Condon E.U., Shortley G.H., 1951, The Theory of Atomic Spectra. Cambridge University Press, London, p. 365
Corliss C., Sugar J., 1982, J. Phys. Chem. Ref. Data 11, 135
Eissner W., Jones M., Nussbaumer H., 1974, Computer Phys. Commun. 8, 270
Fawcett B.C., 1986, ADNDT 35, 203
Flower D.R., 1977, A&A 54, 163
Gabriel A.H., Jordan C., 1975, MNRAS 173, 397
Hummer D.G., Berrington K.A., Eissner W., Pradhan A.K., Saraph H.E., Tully J.A., 1993, A&A 279, 298
Jordan C., 1971, Solar Phys. 21, 381
Jupen C., Isler R.C., Träbert E., 1993, MNRAS 264, 627
Mason H.E., 1994, ADNDT 57, 305
Mason H.E., Monsignori Fossi B.C., 1994, A&A Rev. 6, 123
Nussbaumer H., Storey P.J., 1978, A&A 64, 139
Petrini D., 1970, A&A 9, 392
Saraph H.E., 1972, Computer Phys. Commun. 3, 256
Saraph H.E., Storey P.J., 1996, A&AS 115, 151
Svensson L.Å., 1971, Solar Phys. 18, 232
Tayal S.S., Henry R.J.W., 1986, ApJ 302, 200
Tayal S.S., Henry R.J.W., 1988, ApJ 329, 1023
Tayal S.S., Henry R.J.W., Pradhan A.K., 1987, ApJ 319, 951
Thomas R.J., Neupert W.M., 1994, ApJS 91, 461